IJSRD - International Journal for Scientific Research & Development| Vol. 3, Issue 06, 2015 | ISSN (online): 2321-0613

CFD Analysis of Rear Diffuser in a Sedan Vehicle to Reduce Drag Force

Harish Kulkarni[1] Omprakash.D.Hebbal[2]
[1]M.Tech. Scholar [2]Professor
[1,2]Department of Mechanical Engineering
[1,2]Poojya Doddappa Appa College of Engineering Kalburgi, Karnataka, India

Abstract— The main purpose of this study is to explain the aerodynamic drag reduction mechanism of a passenger car moving at high speed through an actively translating rear diffuser device. In this work nine cases have been defined by varying the length and angle of the diffuser. The angles are varied from 2o to 5o and the length is varied from 50% length to 75% length of the vehicle. Computational Fluid Dynamics (CFD) analysis is performed under moving ground and rotating wheel conditions using ANSYS FLUENT 14.5. The drag co-efficient (CD) value obtained for the primary Sedan model is 0.3562. The minimum drag co-efficient value is obtained for primary Sedan model with the diffuser angle of 5o and 75% length is 0.2792 which is acceptable.

Key words: Rear Diffuser, CFD, Drag Co-Efficient, Sedan Model

I. INTRODUCTION

Nowadays economy will look into a good saving plan by reducing certain aspect of daily activities for example usage of oil and gases in our daily life. Vehicle, aircraft and ship use fuel as a medium to work their role on certain aspect. Petroleum is the main global issue to be discussed in speech, talk and conference.

In addition, the way to reduce the uses of oil and gases is by designing aerodynamic parts and body in order to reduce drag. As the coefficient of drag is low, the better fuel saving as it is more economical [1]. Fuel consumption due to aerodynamic drag consumed more than half of the vehicle’s energy. Thus, the drag reduction program is one of the most interesting approaches to implement this matter. Aerodynamic drag consists of two main components: skin friction drag and pressure drag. Pressure drag accounts for more than 80% of the total drag and it is highly dependent on vehicle geometry due to boundary layer separation from rear window surface and formation of wake region behind the vehicle.

According to Hucho [2], the aerodynamic drag of a road vehicle is responsible for a large part of the vehicle’s fuel consumption and contributes higher fuel consumption at highway speeds. Reducing the aerodynamic drag offers an inexpensive solution to improve fuel efficiency and thus shape optimization for low drag become an essential part of the overall vehicle design process [3]. It has been found that 40% of the drag force is concentrated at the rear of the geometry [4].

The majority of drag in vehicles arises from form drag. Drag force experienced by vehicle is given by equation (1)

$$F_D = ½ \times C_D \times \rho \times A \times U^2, \qquad -(1)$$

Where, C_D is the coefficient of drag, ρ denotes density of air (kg/m^3), A denotes reference area (m^2) and U denotes velocity of the vehicle (m/sec).

The shape of the vehicle uses about 3% of fuel to overcome the resistance in urban driving, while it takes 11% of fuel for the highway driving [5]. This considerable high value of fuel usage in highway driving attracts several design engineers to enhance the aerodynamics of the vehicle. One of the methods is computational fluid dynamics (CFD). The time required for CFD simulations and optimization process depends on many factors including the choice of turbulence model, mesh resolution, the number of design parameters, the parameterization process as well as the optimization strategy.

II. DIFFUSER AND ITS OPERATION

A diffuser, in an automotive context, is an arc shaped section of the car underbody. The diffuser improves the car's aerodynamic properties by enhancing the transition between the high-velocity airflow underneath the car and the much slower freestream airflow of the ambient atmosphere [6]. It works by providing a space for the underbody airflow to decelerate and expand so that it does not cause excessive flow separation and drag, by providing a degree of wake infill or more accurately, pressure recovery. The diffuser itself accelerates the flow in front of it, which helps to generate downforce. The Fig. 1 illustrates the diffuser used in the sedan vehicles by the side and top views.

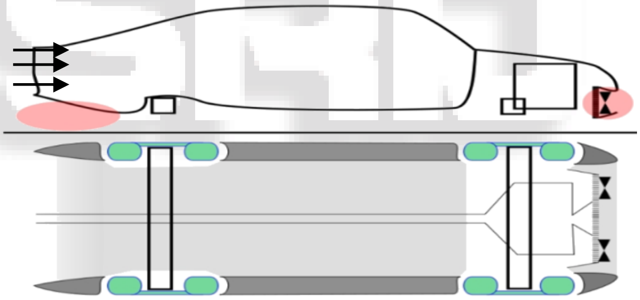

Fig. 1: Diffuser used in the Sedan vehicles

When a diffuser is used, the air flows into the underbody from the front and sides of the car, accelerates and reduces pressure [7]. There is a suction peak at the transition of the flat bottom and diffuser. The diffuser then reduces this high velocity air back to normal velocity and also helps fill in the area behind the car making the whole underbody a more efficient downforce producing device by reducing drag on the car and increasing downforce.

A. *Ahmed body:*

The investigation has obtained the behavior of newly developed turbulence models for complex geometry cases, a simplified car model, known as the Ahmed body, has been tested by Ahmed [8]. Experiments were conducted to investigate the effect of backlight angles in the range of 0^o to 40^o. The backlight angle is the angle of depression of the rear window. Fig. 2 shows a schematic representation of an Ahmed body. In this range, two critical backlight angles (α) which were identified to have a significant influence on the flow structure were 12.5^o and 30^o. Three ranges of backlight angles were identified which have different aerodynamic effects: $0^o<\alpha<12.5^o$; $12.5^o<\alpha<30^o$; and $\alpha>30^o$.In the range of $0^o<\alpha<12.5^o$, the flow remains attached over the rear window slant and separates at the top and bottom edges of the vertical base.

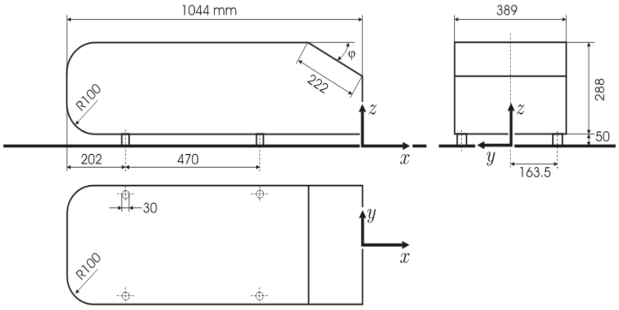

Fig. 2: Schematic representation of an Ahmed body

III. COMPUTATIONAL FLUID DYNAMICS (CFD):

Computational fluid dynamics, usually abbreviated as CFD, is a branch of fluid mechanics that uses numerical methods and algorithms to solve and analyze problems that involve fluid flows. Computers are used to perform the calculations required to simulate the interaction of liquids and gases with surfaces defined by boundary conditions using ANSYS FLUENT 14.5. The technique is very powerful and spans a wide range of industrial and non-industrial areas.

A. Governing Equations

The governing equations of fluid flow represent mathematical statements of the conservation laws of physics:

- The mass of a fluid is conserved
- The rate of change of momentum equals the sum of the forces on a fluid particle (Newton's second law)
- The rate of change of energy is equal to the sum of the rate of heat addition to and the rate of work done on a fluid particle (first law of thermodynamics).

The fluid will be regarded as a continuum. For the analysis of fluid flows at macroscopic length scales the molecular structure of matter and molecular motions may be ignored. We describe the behavior of the fluid in terms of macroscopic properties, such as velocity, pressure, density and temperature, and their space and time derivatives. These maybe thought of as averages over suitably large numbers of molecules [9].

B. Mass Conservation in Three Dimensions

According to conservation of mass law [10], the continuity equation is given by,

$$\frac{\partial\rho}{\partial t}+\frac{\partial(\rho u)}{\partial x}+\frac{\partial(\rho v)}{\partial y}+\frac{\partial(\rho w)}{\partial z}=0 \qquad \text{-(1)}$$

Equation (1) is the unsteady, three-dimensional mass conservation or continuity equation at a point in a compressible fluid. For an incompressible fluid (i.e. a liquid) the density ρ is constant and equation (1) becomes

$$\frac{\partial u}{\partial x}+\frac{\partial v}{\partial y}+\frac{\partial w}{\partial z}=0 \qquad \text{-(2)}$$

C. Momentum Equation in Three Dimensions

According to Newtons law [10], the rate of change of momentum of a fluid particle equals the sum of forces on the particle.

$$\rho\frac{Du}{Dt}=\frac{\partial(-p+\tau_{xx})}{\partial x}+\frac{\partial\tau_{yx}}{\partial y}+\frac{\partial\tau_{zx}}{\partial z}+S_{Mx} \qquad \text{-(3)}$$

Equation (3) is the momentum equation in *x*-direction

$$\rho\frac{Dv}{Dt}=\frac{\partial\tau_{xy}}{\partial x}+\frac{\partial(-p+\tau_{yy})}{\partial y}+\frac{\partial\tau_{zy}}{\partial z}+S_{My} \qquad \text{-(4)}$$

Equation (4) is the momentum equation in *y*-direction

$$\rho\frac{Dw}{Dt}=\frac{\partial\tau_{xz}}{\partial x}+\frac{\partial\tau_{yz}}{\partial y}+\frac{\partial(-p+\tau_{zz})}{\partial z}+S_{Mz} \qquad \text{-(5)}$$

Equation (5) is the momentum equation in *z*-direction. And where the pressure and normal stress is denoted by p and σ. Viscous stresses are denoted by τ. The usual suffix notation τ_{ij} is applied to indicate the direction of the viscous stresses. The suffixes i and j in τ_{ij} indicate that the stress component acts in the j direction on a surface normal to the i direction.

IV. METHODOLOGY

CFD analysis and study of results are carried out in 3 steps: Pre-processing, solving and post-processing. The model of a primary Sedan of HONDA CITY vehicle is been analyzed using various boundary conditions. The different models of the Sedan vehicle have also been analyzed by changing the various angles of the diffuser at different lengths.

Geometry of the CAD model is created in CATIA V5 R20 modeling software [11], and imported into the ANSYS Workbench 14.5. Meshing is carried out using the ANSYS Mesher tool by defining the element size for the fluid domain. Fig. 3 and Fig. 4 show the CATIA geometry and meshing of primary Sedan model respectively. The mesh generated through the ANSYS Mesher tool is imported into the ANSYS FLUENT solver and the solution is simulated for 1000 iterations. Extracted physical quantities like velocities and pressures are displayed by streamline and contour plots.

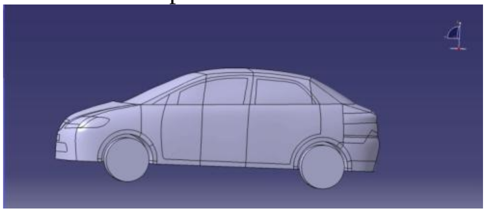

Fig. 3: CATIA primary sedan model of HONDA CITY

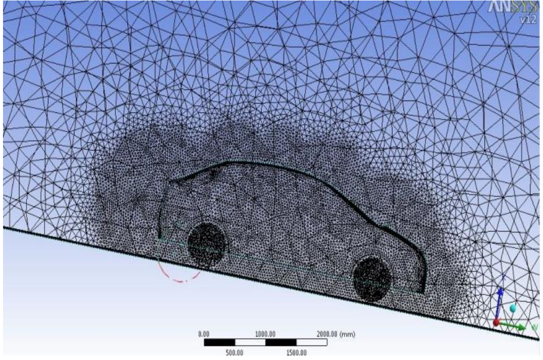

Fig. 4: Meshing of primary sedan model HONDA CITY

Nine cases had been defined by changing the length and angle of the diffuser of the primary Sedan model. The angles are varied from 2^0 to 5^0 with the lengths being measured from 50% length of the vehicle and 75% length of the vehicle in CATIA as shown in table 1.

Case	Diffuser description
1	Primary Sedan model
2	50% length with angle of 2^0
3	75% length with angle of 2^0
4	50% length with angle of 3^0
5	75% length with angle of 3^0
6	50% length with angle of 4^0
7	75% length with angle of 4^0
8	50% length with angle of 5^0
9	75% length with angle of 5^0

Table 1: Different cases by modifying the rear diffuser

A. Boundary Conditions and Case Set Up

The boundary conditions specified in this project are as given in Table 2

Motion	Stationary
Time	Steady State Analysis
Material	Air Flow
Inlet flow velocity	60 m/sec
Design Pressure	Atmospheric
Wheel 1	31.82 rpm (CW)
Wheel 2	31.82 rpm (CW)
Temperature	288 K
Viscous Regime	Turbulent Flow
Turbulence Model	Realizable k-є Model
Road	Moving, Absolute, Transitional with V=60 m/sec
Wall	No slip condition

Table 2: Boundary conditions

B. Realizable K-Epsilon Turbulence Model

The turbulent nature of the flow plays a crucial part in the determination of many engineering parameters, such as frictional drag, flow separation, transition from laminar to turbulent flow, thickness of boundary layers etc. The turbulent states which can be encountered across the whole range of industrially relevant flows are rich, complex and varied [12]. After a century of intensive theoretical and experimental research, it is now accepted that no single turbulence model can span these states and there is no generally valid universal model of turbulence. In the dissipation rate (ε) equation is derived from the mean-square vorticity fluctuation, which is fundamentally different from the standard k-ε model. Several realizability conditions are enforced for Reynolds stresses. The realizable k-є turbulence model is likely to provide superior performance for flows involving rotation, boundary layers under strong adverse pressure gradients, separation, and recirculation [13].

V. RESULTS AND DISCUSSION

Analysis of different cases is carried out in ANSYS FLUENT 14.5 solver. Numerical value of drag co-efficient (C_D) of the primary Sedan model with different cases are obtained.

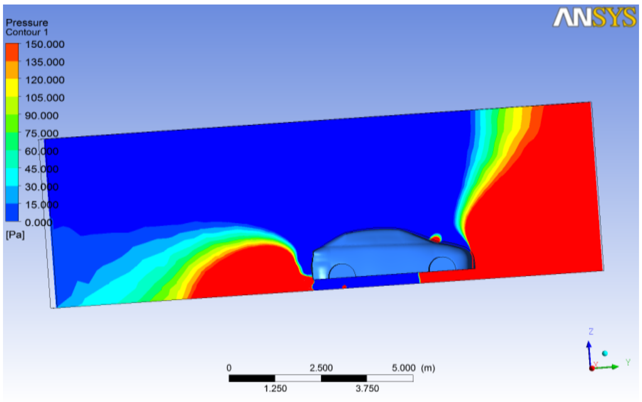

Fig. 5: Pressure contour over the sedan model HONDA CITY

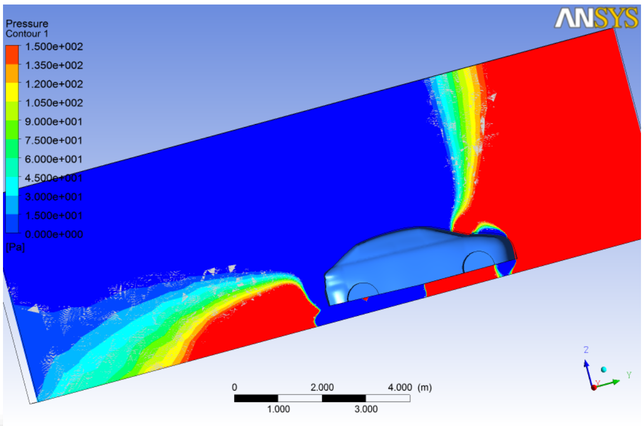

Fig. 6: Pressure contour over the sedan model 50% length with angle of 2^0

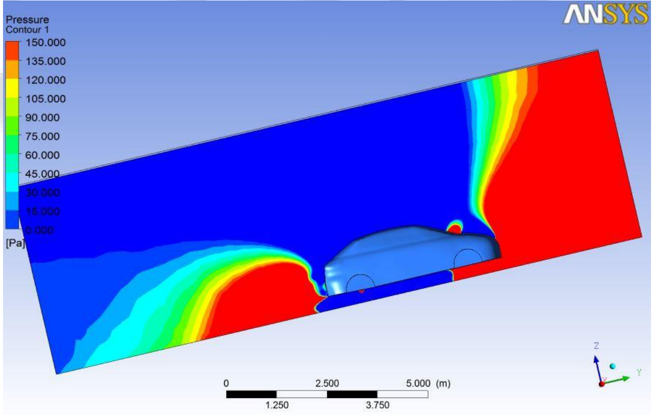

Fig. 7: Pressure contour over the sedan model 75% length with angle of 2^0

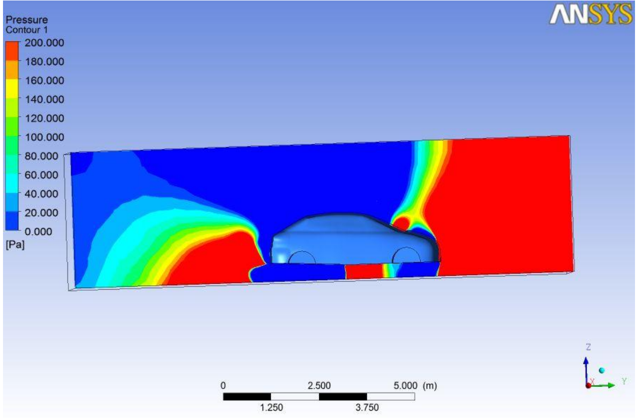

Fig. 8: Pressure contour over the sedan model 50% length with angle of 3^0

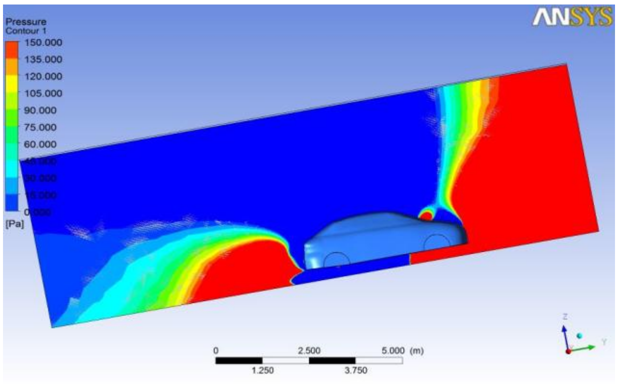

Fig. 9: Pressure contour over the sedan model 75% length with angle of 3^0

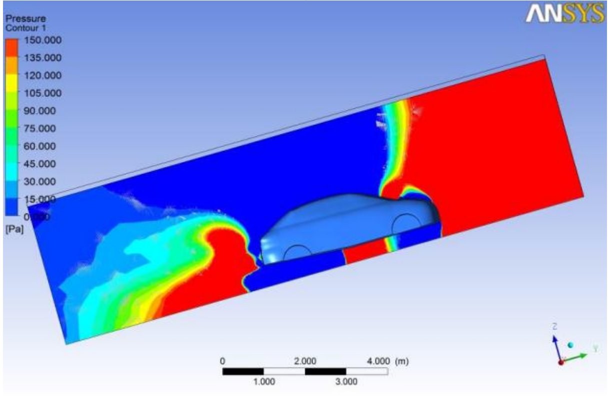

Fig. 10: Pressure contour over the sedan model 50% length with angle of 4^0

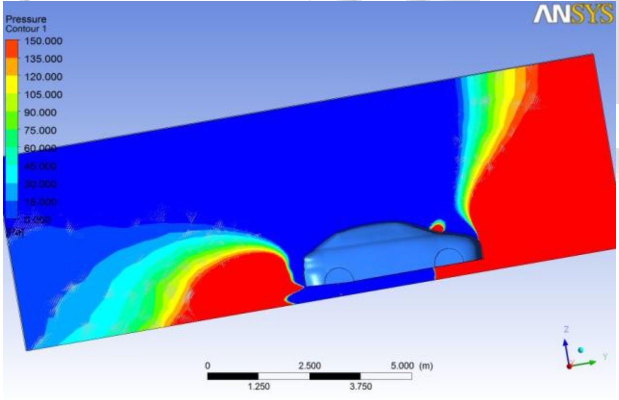

Fig. 11: Pressure contour over the sedan model 75% length with angle of 4^0

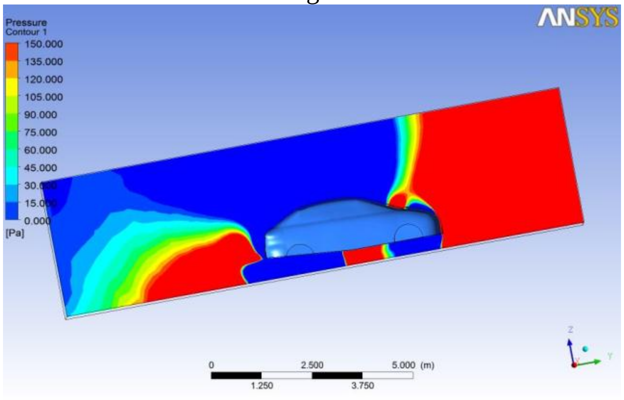

Fig. 12: Pressure contour over the sedan model 50% length with angle of 5^0

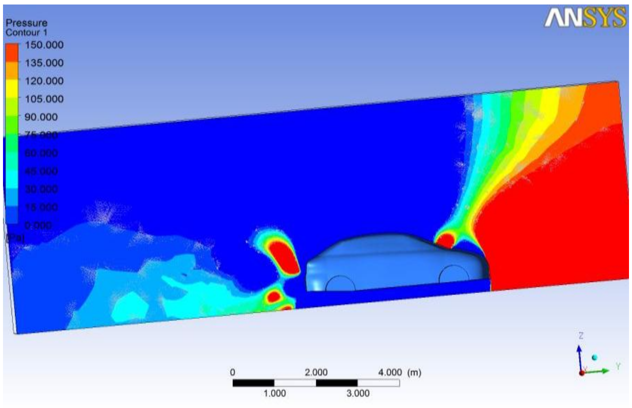

Fig. 13: Pressure contour over the sedan model 75% length with angle of 5^0

The Fig. 5 shows the pressure contour at a velocity of 60 m/sec. The drag co-efficient was found to be C_D=0.3562. The Fig. 6 shows the pressure contour of Sedan of 50% length with angle of 2^0 at a velocity of 60 m/sec. The drag co-efficient was found to be C_D=0.4705. The Fig. 7 shows the pressure contour of Sedan of 75% length with angle of 2^0 at a velocity of 60 m/sec. The drag co-efficient was found to be C_D=0.3184. The Fig. 8 shows the pressure contour of Sedan of 50% length with angle of 3^0 at a velocity of 60 m/sec. The drag co-efficient was found to be C_D=0.3797. The Fig. 9 shows the pressure contour of Sedan of 75% length with angle of 3^0 at a velocity of 60 m/sec. The drag co-efficient was found to be C_D=0.3089. The Fig. 10 shows the pressure contour of Sedan of 50% length with angle of 4^0 at a velocity of 60 m/sec. The drag co-efficient was found to be C_D=0.3711. The Fig. 11 shows the pressure contour of Sedan of 75% length with angle of 4^0 at a velocity of 60 m/sec. The drag co-efficient was found to be C_D=0.2925. The Fig. 12 shows the pressure contour of Sedan of 50% length with angle of 5^0 at a velocity of 60 m/sec. The drag co-efficient was found to be C_D=0.4005. The Fig. 13 shows the pressure contour of Sedan of 75% length with angle of 5^0 at a velocity of 60 m/sec. The drag co-efficient was found to be C_D=0.2792, as the maximum pressure exists far away from the diffuser and also only at the few regions higher pressures are generated in the rear portion when compared to that of the front portion Thus, the total pressure gradient gets reduced drastically and a small wake region is formed when compared to that of the primary sedan model Thus, it can be said that modifying the rear diffuser with an angle of 5^o and providing the cut from the 75% of the length of the vehicle gives the satisfactory results.

The table 3 shows the drag co-efficient values obtained for the primary Sedan model for different cases by changing the length and angles of the rear diffuser.

Case	Diffuser description	C_D
1	Primary Sedan model	0.3562
2	50% length with angle of 2^0	0.4705
3	75% length with angle of 2^0	0.3184
4	50% length with angle of 3^0	0.3797
\5	75% length with angle of 3^0	0.3089
6	50% length with angle of 4^0	0.3711
7	75% length with angle of 4^0	0.2925
8	50% length with angle of 5^0	0.4005
9	75% length with angle of 5^0	0.2792

Table 3: Drag co-efficient (C_D) values of different cases by modifying the rear diffuser

A. Comparison of Drag Co-Efficient with the Experimental Results

An experimental investigation data is collected for the primary Sedan model [14], which showed the drag co-efficient (C_D) value of 0.36, and the results for simulation obtained is C_D=0.3562 and are well comparable. A comparison is made with the experimental results to the primary Sedan model and the other cases, as shown in Fig. 14. Among the various lengths and angles of the diffuser, case 9 (5^o with the 75% of the length of the vehicle) showed the best drag reduction performance, with an average reduction of more than 8%. Moreover, as the driving speed increases, the drag reduction effect also increases.

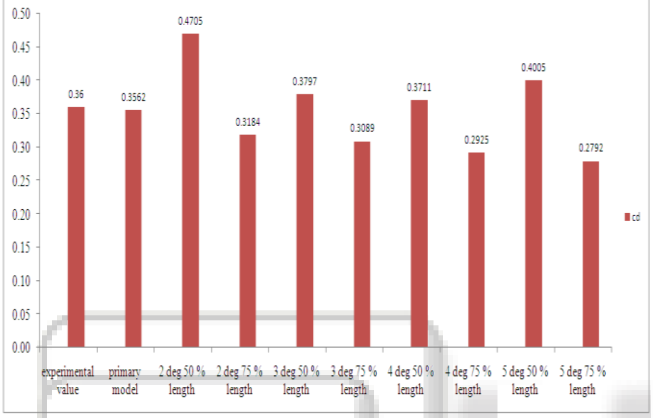

Fig. 14: Comparison of drag co-efficient values of the different models of sedan

VI. CONCLUSIONS

After conducting various analysis of the primary Sedan model and other cases the following conclusions are made,

- In the primary Sedan model the drag co-efficient obtained is 0.3562. The experimental value for the primary Sedan model is 0.36. The experimental value and the analysis values are comparable.
- In the primary Sedan model with the diffuser angle of 2^o and 50% length the drag co-efficient obtained is 0.4705. There is an increase in the drag co-efficient value.
- In the primary Sedan model with the diffuser angle of 2^o and 75% length the drag co-efficient obtained is 0.3184. There is a decrease in the drag co-efficient value.
- In the primary Sedan model with the diffuser angle of 3^o and 50% length the drag co-efficient obtained is 0.3797. There is an increase in the drag co-efficient value.
- In the primary Sedan model with the diffuser angle of 3^o and 75% length the drag co-efficient obtained is 0.3089. There is a decrease in the drag co-efficient value.
- In the primary Sedan model with the diffuser angle of 4^o and 50% length the drag co-efficient obtained is 0.3711. There is an increase in the drag co-efficient value.
- In the primary Sedan model with the diffuser angle of 4^o and 75% length the drag co-efficient obtained is 0.2925. There is a decrease in the drag co-efficient value.
- In the primary Sedan model with the diffuser angle of 5^o and 50% length the drag co-efficient obtained is 0.4005. There is an increase in the drag co-efficient value.
- In the primary Sedan model with the diffuser angle of 5^o and 75% length the drag co-efficient obtained is 0.2792. There is a decrease in the drag co-efficient value.
- It is also observed that drag co-efficient was reduced only for the 75% length of the vehicle compared to 50% length of the vehicle.

Thus, we can conclude that in the primary Sedan model with diffuser angle of 5^o and 75% length, the drag co-efficient is minimum and is acceptable.

REFERENCES

[1] Krishnani, P. N. (2009) CFD study of drag reduction of a generic sport utility vehicle, *Master's Thesis*, Mechanical Engineering Department, California State University, Sacramento.
[2] Hucho, W. H. and Sovran, G. (1993) Aerodynamics of road vehicles, Annual Review of Fluid Mechanics, Vol. 25(1), pp485-537.
[3] Mayer, W., and Wickern, G. (2011) The new audi A6/A7 family-aerodynamic development of different body types on one platform, SAE International Journal of Passenger Cars-Mechanical Systems, Vol. 4(1), pp197-206.
[4] Chainani. A, and Perera. N, (2008) CFD Investigation of airflow on a model radio control race car, *WCE 2008*, 2-4July, London.
[5] CFD Analysis of Aerodynamic Drag Reduction of Automobile Car - A Review. International Journal of Science and Research (IJSR) Volume 3 Issue 6, June 2014
[6] Review of Research on Vehicles Aerodynamic Drag Reduction Methods. International Journal of Mechanical & Mechatronics Engineering IJMME-IJENS Vol: 14 No: 02
[7] JESPER MARKLUND, Under-body and Diffuser Flows of Passenger Vehicles Department of Applied Mechanics CHALMERS UNIVERSITY OF TECHNOLOGY ISBN 978-91-7385-866-3
[8] CFD Aerodynamic Analysis of Ahmed Body, International Journal of Engineering Trends and Technology (IJETT) – Volume 18 Number 7 – Dec 2014.
[9] An Introduction to Computational Fluid Dynamics, ”THE FINITE VOLUME METHOD” Second Edition by H K Versteeg and W Malalasekera.
[10] “Advanced engineering fluid mechanics”, Second edition by K.Muralidhar and Gautam Biswas
[11] www.grabcaed/sedan/hondacity.com
[12] ACTIVELY TRANSLATING A REAR DIFFUSER DEVICE FOR THE AERODYNAMIC DRAG REDUCTION OF A PASSENGER CAR. International Journal of Automotive Technology, Vol. 13, No. 4, pp. 583−592 (2012)
[13] Simon Watkins, Gioacchino Vino "The effect of vehicle spacing on the aerodynamics of a representative car

shape" Journal of Wind Engineering and Industrial Aerodynamics 96 (2008) p.1232–1239

[14] Experimental Studies on The Effect Of Drag Acting On Car Windscreens, https://windshieldcapstoneemd4713.wordpress.com/